Pergamon

Geochimica et Cosmochimica Acta, Vol. 60, No. 14, pp. 2651–2666, 1996

0016-7037/96 $15.00 + .00

PII S0016-7037(96)00116-0

Indicators of aqueous alteration and thermal metamorphism on the CV parent body: Microtextures of a dark inclusion from Allende

TOMOKO KOJIMA[1,*] and KAZUSHIGE TOMEOKA[2]

[1] Mineralogical Institute, Graduate School of Science, University of Tokyo, Hongo, Bunkyo-ku, Tokyo 113, Japan
[2] Department of Earth and Planetary Sciences, Faculty of Science, Kobe University, Nada, Kobe 657, Japan

(*Received August* 4, 1995; *accepted in revised form March* 26, 1996)

Abstract—An unusual dark clast in the Allende CV3 chondrite (termed Allende-AF), which was previously interpreted as a primary aggregate formed in the solar nebula (Kurat et al., 1989; Palme et al., 1989), was re-examined. Our study reveals abundant evidence suggesting that it probably experienced extensive aqueous alteration and subsequent thermal metamorphism on the meteorite parent body. Allende-AF contains numerous rounded to oval-shaped inclusions embedded in a dark matrix. The inclusions, consisting predominantly of fine grains of Fe-rich olivine, have internal textures suggesting that they are pseudomorphs after chondrules. Several inclusions appear to be replaced CAIs. Veins filled with fibrous olivine grains occur abundantly in both inclusions and matrix; some veins (up to 4 mm in length) penetrate several inclusions, providing strong evidence that aqueous alteration occurred after accretion. The fibrous morphology of olivine in veins and inclusions suggests that the olivine was produced by dehydration and thermal transformation of phyllosilicate that had been formed by aqueous alteration. Olivine grains in the matrix contain numerous micro-inclusions of Fe-Ni sulfide, which were probably incorporated during transformation from phyllosilicate.

Allende-AF is probably related to the fine-grained variety of dark inclusions reported from CV3 chondrites that has been described as the type containing abundant porous aggregates of Fe-rich olivine by Johnson et al. (1990). Many dark inclusions previously described appear to be similar in texture and mineralogy to Allende-AF, and probably experienced similar secondary process on the meteorite parent body. The wide variation in texture of dark inclusions can be explained by different degrees of aqueous alteration that preceded thermal metamorphism.

The size distribution of chondrule pseudomorphs and the abundance of CAI pseudomorphs suggest that the precursor of Allende-AF is a CV type chondrite, probably Allende itself. Oxygen isotopic and chemical compositions are consistent with this interpretation. The CV parent body has been commonly thought to have escaped major secondary processing. However, Allende-AF provides evidence that extensive aqueous alteration and thermal metamorphism have occurred locally on the CV parent body.

1. INTRODUCTION

Dark inclusions (DIs) commonly occur in Allende and, less commonly, in some other CV3 carbonaceous chondrites. They are lithic clasts that range in size from 1 mm to several centimeters and widely range in texture; one endmember is composed of chondrules and CAIs embedded in a fine-grained matrix resembling host CV3 meteorites, and the other endmember consists mostly of fine grains of homogeneous Fe-rich olivine (e.g., Fruland et al., 1978; Johnson et al., 1990) and lacks chondrules, CAIs, and coarse mineral fragments. Most DIs have textures that are intermediate between these two endmembers, i.e., they vary in amount of the fine-grained component. Despite the textural variations, most DIs are similar in chemical and oxygen isotopic compositions to CV3 chondrites (Fruland et al., 1978; Bischoff et al., 1988; Johnson et al., 1990), suggesting that they are fragments of a common CV parent body.

The origin of DIs has been a subject of controversy; they have been proposed to be (1) primary aggregates of condensates from the solar nebula (Kurat et al., 1989; Palme et al., 1989), (2) fragments of CV3 parent bodies which were processed to different degrees by reaction with the solar nebula gas prior to their incorporation into the host meteorites (Johnson et al., 1990), and (3) CV3 materials that were affected by various degrees of thermal metamorphism on their parent bodies (Bunch and Chang, 1979, 1983). DIs consist largely of fine-grained materials texturally and mineralogically similar to the matrices of CV3 and CO3 chondrites. Mainly for this reason, most previous workers favored the interpretation that DIs represent primitive materials formed in the solar nebula (Bischoff et al., 1988; Kurat et al., 1989; Palme et al., 1989; Johnson et al., 1990).

Recently, however, Kojima et al. (1993) studied two unusual DIs in the Vigarano CV3 chondrite and found evidence suggesting that the DIs have experienced aqueous alteration and subsequent thermal metamorphism on the meteorite parent body. The DIs in Vigarano contain no chondrules and CAIs, but instead contain rounded to oval-shaped aggregates similar in size and shape to chondrules that are composed of fine Fe-rich olivine grains. Kojima et al. (1993) interpreted that the aggregates are pseudomorphs after chondrules. They also suggested that the fine grains of Fe-rich olivine that constitute the major part of the DIs were produced by dehydration and thermal transformation of phyllosilicates that had been formed by aqueous alteration.

Rounded to oval-shaped aggregates of Fe-rich olivine that are similar to chondrules have been reported also from other DIs (Johnson et al., 1990). In particular, Kurat et al. (1989)

*Present address: Department of Earth and Planetary Sciences, Faculty of Science, Kobe University, Nada, Kobe 657, Japan.

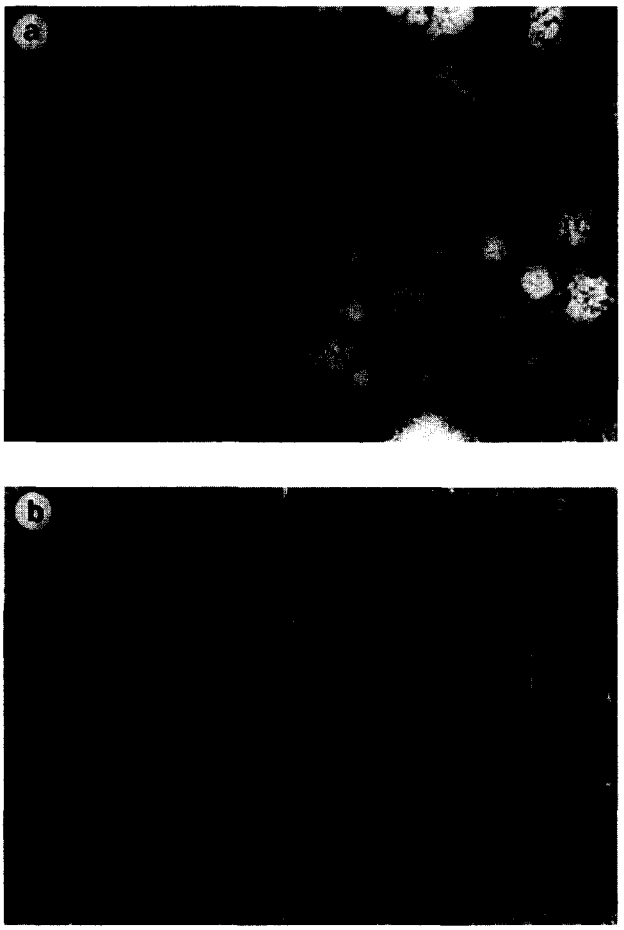

FIG. 1. (a) A portion around the boundary between All-AF (left) and host Allende (right) in plane polarized light. Inclusions in All-AF are similar in shape and size to chondrules and chondrule fragments in host Allende, but differ in that they are brownish translucent. (b) Backscattered electron (BSE) image of the same portion as in (a) on the same scale. The boundary is marked by a broken line.

and Palme et al. (1989) reported in detail such aggregates occurring in a clast from Allende (termed "Allende-AF" by them). From their descriptions, Allende-AF appears to be very similar to the Vigarano DIs that Kojima et al. (1993) reported. However, the interpretation of Kurat et al. (1989) and Palme et al. (1989) for the origin of Allende-AF is very different from that of Kojima et al. (1993). Kurat et al. (1989) and Palme et al. (1989) interpreted Allende-AF to be a primary aggregate of direct condensates from a nebular gas, and that the rounded to oval-shaped aggregates are precursors of chondrules, which would transform to chondrules by sintering, recrystallization, and partial melting in the solar nebula.

Through the courtesy of Professor G. Kurat, we were granted an opportunity to re-examine Allende-AF and to compare it with the DIs in Vigarano. The main purpose of this study is to verify whether Allende-AF is really a primitive aggregate of nebular condensates as interpreted by Kurat et al. (1989) and Palme et al. (1989), or a product of parent body process as interpreted by Kojima et al. (1993). Our detailed petrographic and scanning electron microscope (SEM) study reveals several lines of new evidence supporting that Allende-AF has experienced aqueous alteration and subsequent thermal dehydration on the CV parent body, and thus has a formation history similar to the DIs in Vigarano. Our preliminary results have been reported in Kojima and Tomeoka (1993, 1994). We believe that Allende-AF as well as the Vigarano DIs provide new information regarding the secondary processes that occurred on the CV parent bodies.

2. MATERIALS AND METHODS

Allende-AF (hereafter All-AF) has a rectangular cross section of about 1 × 2 cm extending through several slices of 0.8 cm thickness each (Kurat et al., 1989). The total volume of the inclusion amounts to 3 cm^3. A polished thin section (5.8 cm^2 total area) and a small chip containing All-AF provided by Professor G. Kurat, Naturhistorisches Museum, were used in this study. All-AF is approximately 12 × 18 mm and 4 × 8 mm in size in the two thin sections. The thin sections were examined with an optical microscope and scanning electron microscopes (JEOL JSM-840 and JSM-5800) equipped with energy-dispersive X-ray spectrometers (EDS). EDS analyses were obtained at 15 kV and 1.0 nA, and corrections were made by ZAF method. Well-characterized natural and synthetic minerals and glasses were used as standards. The accuracy of the EDS analyses was checked by comparison with data obtained by EPMA for the same materials, and the results agreed within a range of 1% error for elements present in more than 1.0 wt%. For the analysis of each mineral grain, we used a focused electron beam of 2 μm in diameter. Bulk compositions of All-AF were determined using a defocused electron beam of 100 μm in diameter. Compositions of inclusions and matrix in All-AF were also obtained by the same method.

3. TEXTURE AND MINERALOGY

3.1. General Petrography

All-AF consists of numerous rounded to oval shaped inclusions (<0.1 to 2.5 mm in diameter) embedded in a dark matrix (Figs. 1a, 2). The inclusions are similar in shape and size to chondrules or chondrule fragments in the host meteorite, and some resemble CAIs. Thus, under the optical microscope, All-AF has an appearance similar to host Allende except that the inclusions are brownish and translucent. Many of the inclusions are flattened with aspect ratios from

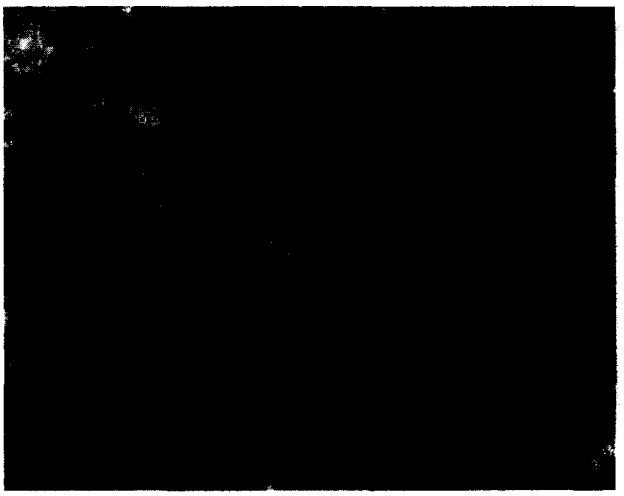

FIG. 2. A portion of All-AF in plane polarized light. Note that inclusions located near the Inclusion I-1 (marked by a broken line) are flattened roughly along the surface of Inclusion I-1.

Table 1. EDS broad beam analyses (100 μm in diameter) of Allende-AF (weight %).

	All-AF Bulk		Chondrule-like inclusion		CAI-like inclusion		Matrix		All-AF rim		Allende host * Matrix	Allende host #Bulk
N	136	(sd)	36	(sd)	10	(sd)	38	(sd)	36	(sd)	—	—
SiO_2	29.2	(4.4)	29.8	(2.0)	24.0	(8.8)	29.0	(1.8)	27.5	(2.6)	28.0	29.0
Al_2O_3	4.18	(2.17)	2.90	(1.08)	6.67	(3.53)	3.85	(1.41)	1.84	(0.45)	2.30	2.77
TiO_2	0.30	(0.53)	0.18	(0.06)	1.55	(1.26)	0.11	(0.06)	0.18	(0.09)	0.09	0.13
FeO	24.1	(6.1)	24.5	(3.2)	32.0	(17.6)	24.0	(2.7)	31.7	(5.7)	31.9	25.6
MnO	0.26	(0.07)	0.29	(0.29)	0.20	(0.08)	0.27	(0.06)	0.36	(0.07)	0.21	0.16
MgO	21.9	(4.6)	24.5	(2.3)	9.88	(5.43)	23.1	(2.3)	17.1	(2.1)	20.2	20.8
CaO	2.27	(3.55)	1.08	(0.74)	9.37	(7.20)	1.05	(1.99)	3.43	(2.66)	2.37	2.18
Na_2O	0.89	(1.03)	0.33	(0.42)	1.64	(1.31)	0.74	(0.73)	0.17	(0.20)	0.22	0.39
K_2O	0.09	(0.07)	0.06	(0.04)	0.16	(0.11)	0.07	(0.04)	0.03	(0.01)	0.01	0.03
Cr_2O_3	0.55	(0.22)	0.66	(0.21)	0.20	(0.09)	0.54	(0.15)	0.58	(0.14)	0.38	0.45
NiO	1.34	(0.87)	1.57	(1.25)	0.47	(0.19)	1.27	(0.56)	1.46	(0.43)	1.83	1.53
P_2O_5	0.11	(0.16)	0.04	(0.08)	0.07	(0.14)	0.17	(0.20)	0.24	(0.22)	n. a.	0.20
S	1.50	(3.08)	1.01	(1.04)	7.45	(9.65)	1.00	(0.50)	2.27	(0.87)	1.13	1.77
Total	86.7		86.9		93.7		85.2		86.9		88.6	85.0

N=number of analyses. n. a.=not analyzed. sd=standard deviations.

* From McSween and Richardson (1977). Data obtained by WDS defocused beam (100 μm in diameter) analysis.

From Jarosewich *et al.* (1987). Normalized to total 85 %.

1.5 to 2.0; the flattening occurs locally in the same direction (Fig. 2). Fracture-filling veins of various thicknesses and lengths occur throughout this clast; they occur in both inclusions and matrix and are particularly abundant in the peripheries of relatively large inclusions, as described later.

Under the SEM, differences between All-AF and host Allende are more obvious. All-AF is composed mainly of fine grains of Fe-rich olivine that are uniform in size and composition, giving a very homogeneous appearance (Fig. 1b). The boundaries between inclusions, veins, and matrix are hardly discernible, which contrasts with the host meteorite in which chondrules, CAIs, and matrix are easily distinguishable. Olivine grains in All-AF are distinctly coarser (mostly 5 to 10 μm in diameter) than those in the matrix of host Allende (mostly <1 to 5 μm).

The boundary between All-AF and host Allende is sharp and is marked by a discontinuous rim ranging in thickness from 20 to 200 μm. The rim consists mainly of fine grains of Fe-rich olivine which are similar in size (<1 to 5 μm in diameter) and composition to those in the matrix of host Allende. In some portions, the boundary between the rim and host Allende is not sharp. The rim contains higher amounts of Fe sulfide and Ca-Mg-rich silicate, probably Ca-rich pyroxene, than the Allende matrix, which is reflected in the higher contents of Ca and S than the latter (Table 1). The part of the rim next to the extraordinarily large inclusion (Inclusion I-1; described later) is particularly enriched in tiny grains (<1 μm) of Fe sulfide.

Based on the textural characteristics, we classify the components of All-AF as follows: (1) chondrule-like inclusions, (2) CAI-like inclusions, (3) matrix, and (4) veins. The texture and mineralogy of each component are described in detail in the following sections.

3.2. Chondrule-Like Inclusions

Most inclusions in All-AF are porous aggregates composed mainly of fine grains (<1 to 20 μm in diameter) of Fe-rich olivine (25 to 33 wt% FeO) (Table 2). They also contain minor amounts of a Na-Al-Si-rich phase and lesser amounts of Ca-rich pyroxene. The Na-Al-Si-rich phase appears to be related to nepheline, as described later. These inclusions probably correspond to the "common silicate-rich objects" described by Kurat et al. (1989), who subdivided them into four types: (1) isolated fluffy olivine stacks, (2) olivine aggregates, (3) complex silicate-rich aggregates, and (4) aggregates of complex aggregates. All of the four types were also observed in the present study. The most common are the ones corresponding to the "complex silicate-rich aggregates." We found most of them to be composed of assemblages of rounded to oval-shaped sections (typically 50 to 100 μm in diameter), each consisting of fine grains of olivine (Fig. 3a,c). In some of such inclusions, fine, lath-like grains of olivine (up to 5 μm in width and 20 μm in length) are oriented almost parallel to each other, and the outline of each section is well defined. These sections are most clearly discernible in crossed polarized light. The oriented olivine grains within each section exhibit parallel extinction, indicating that they have a common crystallographic orientation (Figs. 3b, 4a,b). Some rounded sections consist of intimate mixtures of fine grains of olivine and Fe-Ni sulfide; they are nearly opaque in transmitted light, resembling Fe-Ni metal or sulfide globules that commonly occur in chondrules. Some inclusions contain thick bars (5 to 30 μm in width, 100 to 500 μm in length) composed of fine grains of olivine. Bars in an inclusion are oriented parallel to each other and, in crossed polarized light, show the same interference color (Fig. 4a,b), exhibiting an appearance similar to barred olivine chondrules.

Olivine in the chondrule-like inclusions commonly occurs as blocky or lath-like grains (<1 to 20 μm in diameter) which are smooth on the surfaces (Fig. 5a), but it also occurs as fine fibrous grains partly filling interstices between the blocky or lath-like grains. The olivine differs in morphology, size, and associated minerals from that in the matrix of All-AF (described later) (Fig. 5b) and host Allende (Fig. 5c). The morphologies and average grain sizes vary widely between inclusions. Electron beam analyses of olivine in the chondrule-like inclusions show variable amounts of minor elements such as Ca, Al, and Cr; some show unusually high contents of these elements (Table 2, Fig. 6). Although these

Table 2. Selected electron microprobe analyses of olivine in Allende-AF (weight %)*.

	Chondrule-like inclusion					Matrix				Type-II vein	
	1	2	3	4	5	6	7	8	9	10	11
SiO_2	34.8	35.5	35.2	35.7	35.4	36.3	34.0	36.0	34.1	36.8	36.0
Al_2O_3	0.47	0.78	0.59	0.46	0.25	1.20	1.83	1.36	0.95	1.63	1.64
TiO_2	0.41	0.18	0.19	0.21	0.20	0.06	0.11	0.10	0.12	0.15	0.22
FeO	32.3	30.7	31.0	31.6	30.9	28.3	28.8	29.4	32.5	26.6	28.4
MnO	0.21	0.29	0.28	0.30	0.31	0.21	0.37	0.32	0.27	0.43	0.49
MgO	29.4	31.6	31.4	30.7	31.5	31.6	32.1	31.3	30.0	33.7	31.6
CaO	0.78	0.14	0.07	0.17	0.15	0.22	0.23	0.17	0.13	0.46	0.28
K_2O	n. d.	n. d.	n. d.	0.08	0.05	n. d.	n. d.	n. d.	n. d.	n. d.	0.07
Cr_2O_3	0.48	0.55	0.51	0.28	0.37	0.33	0.47	0.41	0.31	n. d.	0.41
NiO	0.47	0.31	0.31	0.37	0.52	0.90	1.04	0.55	0.63	0.38	0.14
S	n. d.	n. d.	n. d.	n. d.	0.08	0.90	0.92	0.34	0.47	0.42	0.37
Total	99.3	100.1	99.6	99.9	99.7	100.0	99.9	100.0	99.5	100.6	99.6
Si	5.81	5.80	5.80	5.88	5.82	5.84	5.42	5.82	5.61	5.83	5.83
Al	0.09	0.15	0.12	0.09	0.05	0.23	0.34	0.26	0.18	0.30	0.31
Ti	0.05	0.02	0.02	0.03	0.03	0.01	0.01	0.01	0.02	0.02	0.03
Fe	4.50	4.20	4.27	4.35	4.26	3.80	3.85	3.97	4.47	3.52	3.84
Mn	0.03	0.04	0.04	0.04	0.04	0.03	0.05	0.04	0.04	0.06	0.07
Mg	7.34	7.72	7.71	7.52	7.73	7.57	7.64	7.54	7.36	7.95	7.62
Ca	0.14	0.03	0.01	0.03	0.03	0.04	0.04	0.03	0.02	0.08	0.05
K	n. d.	n. d.	n. d.	0.02	0.01	n. d.	n. d.	n. d.	n. d.	n. d.	0.01
Cr	0.06	0.07	0.07	0.04	0.05	0.04	0.06	0.05	0.04	n. d.	0.05
Ni	0.06	0.04	0.04	0.05	0.07	0.12	0.13	0.07	0.08	0.05	0.02
S	n. d.	n. d.	n. d.	n. d.	0.01	0.27	0.27	0.10	0.14	0.13	0.11

n. d.=not detected. Atomic ratios are calculated as O=24.
* S, Ni, parts of Fe and minor elements are probably from microinclusions; see text.

olivines rarely contain Fe-Ni-S-rich microinclusions that are resolvable by SEM (>0.05 μm in diameter), the high contents of Ca, Al, and Cr may be ascribed to micro-inclusions that are too small to be observed by SEM.

The second most abundant phase in the inclusions is a phase rich in Na, Al, and Si (14 to 17 wt% Na_2O, 33 to 35 wt% Al_2O_3, 40 to 44 wt% SiO_2) (Table 3). It occurs in almost all the inclusions as anhedral grains (<1 to 10 μm in diameter) partly filling the interstices of olivine grains. Kurat et al. (1989) reported this phase as nepheline, but it should be noted that the contents of Na and K are consistently lower than for nepheline stoichiometry ((Na + K)/total O atomic ratio is approximately 0.18; that for nepheline is 0.25). Whether this is due to Na evaporation during analysis, or the presence of other phases is not clear. Admitting this discrepancy, we call this phase nepheline in this paper. The nepheline contains 1.5 to 2.0 wt% K_2O and 1.8 to 2.9 wt% CaO. Some inclusions contain relatively large (up to 30 μm in diameter) grains of aluminous diopside (17 to 22 wt% CaO, 0.8 to 3.8 wt% Al_2O_3, 0.7 to 1.1 wt% TiO_2) (Table 3) commonly enclosed by thin rims (<5 μm in thickness) of olivine. In some inclusions, aluminous diopside occurs along the rims of the rounded sections described above. Pentlandite occurs in some of the rounded sections and occasionally coexists with awaruite (Table 4). Troilite is present but is much less abundant, and Ni-poor metal is absent.

Many inclusions have rims (20 to 150 μm in thickness) which are distinctly darker than the inclusions and the matrix in transmitted light (Fig. 7). The rims have relatively smooth round external shapes unrelated to the outlines of the inclusions, i.e., they are thickest around topographic depressions of the inclusions, being similar to the fine-grained chondrule rims in carbonaceous chondrites (e.g., Metzler et al., 1992). In some inclusions, boundaries between inclusions and dark rims are partly marked by tiny grains (<5 μm in diameter) of Fe sulfide and/or Fe-Ni metal. The rims are composed of olivine grains that are different in morphology from those in the inclusions but similar to those in the matrix of All-AF (described later). Olivine grains in the rims are slightly smaller and more uniform in size than those in the matrix.

3.3. CAI-Like Inclusions

Six inclusions in the two thin sections of All-AF have mineralogies and textures that are distinct from the chondrule-like inclusions but common to each other. These inclusions are composed mainly of troilite and andradite, corresponding to the "sulfide-andradite objects" described by Kurat et al. (1989). They are triangular to highly irregular in shape (0.5 to 5 mm in diameter) (Fig. 8a). Typically these inclusions contain massive troilite cores which are surrounded by coarse grains (up to 100 μm in diameter) of andradite and/or fine-grained mixture of andradite, Fe-rich olivine, and nepheline. One of the six inclusions contains magnetite instead of troilite (Table 4). Andradite grains occasionally show euhedral shapes (See Fig. 13 in Kurat et al., 1989). Small grains (up to 10 μm in diameter) of Ca-phosphate, Ca-rich pyroxene, and titanomagnetite are commonly included in troilite and andradite. Aggregates of fibrous Fe-rich olivine also occur in voids between andradite grains. Two of the six inclusions have narrow, continuous rims (up to 20 μm in thickness) composed mainly of Ca-rich pyroxene and nepheline (Fig. 8a,b), while others have halos consisting of densely packed olivine with a characteristic fibrous morphology (Fig. 9a,b). The external shape, the core-mantle-rim structure and the high abundances of Ca, Al, and Ti (Table 1) suggest that these inclusions are related to CAIs.

The massive troilite occasionally contains minor amounts

FIG. 3. (a) BSE image of a portion of a chondrule-like inclusion. (b) The same portion as in (a) in crossed polarized light. (c) An illustration showing rounded to oval-shaped sections in the inclusion. Labelled sections correspond to those in (b). Note that sections A, B, and C are in maximum brightness in (b), while sections D and E extinct. Section F is rich in Fe-Ni metal or sulfide (bright areas in (a)) and appears almost opaque in transmitted light.

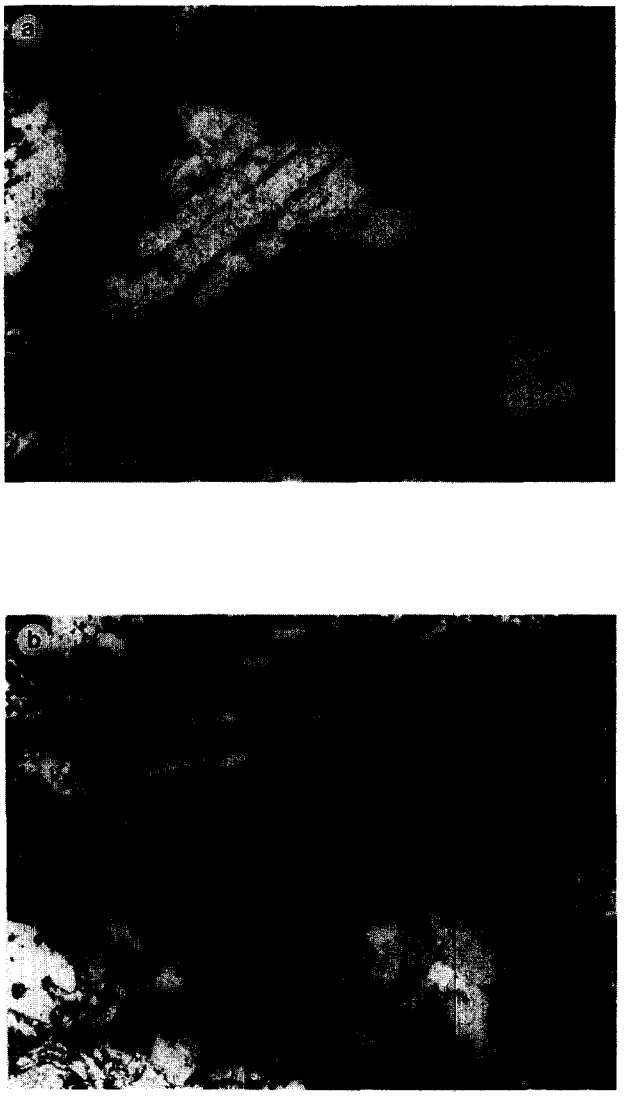

FIG. 4. (a) Two inclusions in All-AF, one (upper left) resembling a fragment of a barred olivine chondrule, and the other (lower right) resembling a porphyritic chondrule in crossed polarized light. (b) 30°-rotated image of the same area. Both inclusions are aggregates of extremely fine grains of olivine. Note that olivine grains in all the bars of the barred-chondrule-like inclusion and olivine grains in several sections of the porphyritic-chondrule-like inclusion go extinct almost simultaneously.

of Si and P (Table 4) which may be due to micro-inclusions. Andradite in the mantle usually contains 1.2 to 1.8 wt% Al_2O_3 (Table 3). Ca-rich pyroxene in the rims contains 9.5 to 14 wt% FeO, while Ca-rich pyroxene included in andradite is distinctly poorer in Fe (7.8 to 8.2 wt% FeO). The nepheline and olivine in the CAI-like inclusions are similar in composition to those in the chondrule-like inclusions. Kurat et al. (1989) reported a variety of unusual accessory phases such as Cu, PGE nuggets, HgS, and barite from the "sulfide-andradite objects," but no such phases were found in the present study.

Inclusion I-1 is by far the largest (5 × 3 mm) of the inclusions and is apparently a broken fragment of an even larger one; its broken surface is in direct contact with host Allende via the rim enclosing All-AF. Inclusion I-1 has an unusually thick, double-layered rim (Fig. 10a,b); the inner layer (up to 200 μm in thickness) consists of a mixture of extremely fine grains (<1 μm) of Fe-rich olivine and

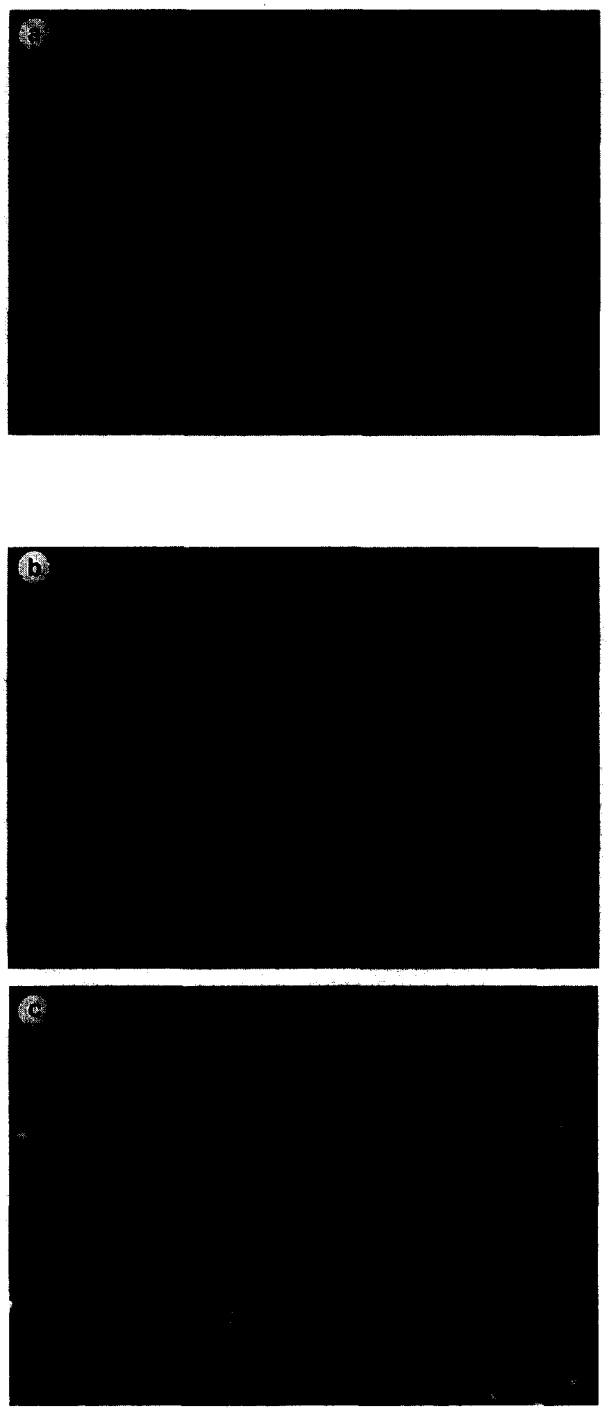

FIG. 5. High-magnification BSE images of portions of a chondrule-like inclusion (a), the matrix of All-AF (b), and the matrix of host Allende (c). All on the same scale.

nepheline, and the outer layer (up to 300 μm thick) consists mainly of granular grains of Fe-rich olivine that are much coarser (up to 30 μm in diameter) than the matrix of All-AF. Interestingly, most of the chondrule-like inclusions near Inclusion I-1 are flattened and aligned along its surface, exhibiting an appearance that they were squashed by intrusion of Inclusion I-1 (Fig. 2). Long, thick veins are particularly abundant around this inclusion (Fig. 11); they tend to be aligned along the surface of the inclusion, again suggesting that considerable mechanical stress was developed and thus many fractures were produced in this region.

3.4. Matrix of All-AF

Although Kurat et al. (1989) described little about the matrix of All-AF, several important features deserve mention. The matrix consists predominantly of olivine grains that are similar in Fe/Mg ratio and size to those in the inclusions. However, the olivine grains in the matrix of All-AF show a characteristic morphology and texture distinct from those in the inclusions; most of them have granular to anhedral shapes, numerous pits, and rough surfaces (Fig. 5b; compare to Fig. 5a). Blocky or fibrous grains similar to the olivine grains in the inclusions also occur but in very minor amounts. Nepheline is more abundant than in the inclusions and fills the interstices between olivine grains.

EDS focused electron beam analyses show that most of the granular olivine grains in the matrix contain considerable amounts of unusual elements such as S, Ni, Al, and Ca (Table 2; Fig. 6), which are usually incompatible in olivine; peculiar is the high, correlated contents of S (up to 1.7 wt% S) and Ni (up to 1.6 wt% NiO) (Table 2; Fig. 6). High-magnification SEM images reveal that most olivine grains in the matrix are not homogeneous but contain numerous micro-inclusions (<0.2 μm in diameter) (Fig. 12). Most of the micro-inclusions are found to be rich in Fe, S, and Ni; thus, they probably consist of Fe-Ni sulfide. The high Al and Ca contents also may be due to micro-inclusions. For minor elements other than the above elements, there are no significant differences between olivines in the chondrule-like inclusions and in the matrix except for Cr; olivines in the matrix are apparently depleted in Cr (<0.5 wt% Cr_2O_3) compared with those in the chondrule-like inclusions (Fig. 6).

3.5. Veins

Based on texture and size, veins are classified into two types. Type-I veins, which range widely in width from several to 100 μm and in length from 0.3 to 1 mm, occur throughout the matrix, but are particularly abundant in the peripheries of relatively large chondrule-like and CAI-like inclusions (Fig. 11). The veins are densely filled with fine fibrous grains of olivine most of which are oriented nearly normal to the walls of the veins (Fig. 13a). The texture is very similar to the phyllosilicate veins found in the Yamato-82162 CI chondrite (compare to Fig. 1 in Tomeoka, 1990). Nepheline occurs in minor amounts in the interstices between the fibrous olivine grains. The type-I veins tend to extend nearly parallel to the surfaces of the inclusions (Fig. 11), and some occur on the boundaries between the inclusions and the matrix. Some veins branch out to narrower veins, forming a network. Kurat et al. (1989) briefly reported that cracks in All-AF are filled with fibrous olivines, which probably correspond to type-I veins.

Type-II veins are narrower (<30 μm in width) and more uniform in width but much longer; all veins longer than 2 mm are of this type. They occur throughout All-AF and are particularly abundant around the CAI-like inclusions, and probably correspond to the "large bended olivine plates" described by Kurat et al. (1989). Particularly striking feature

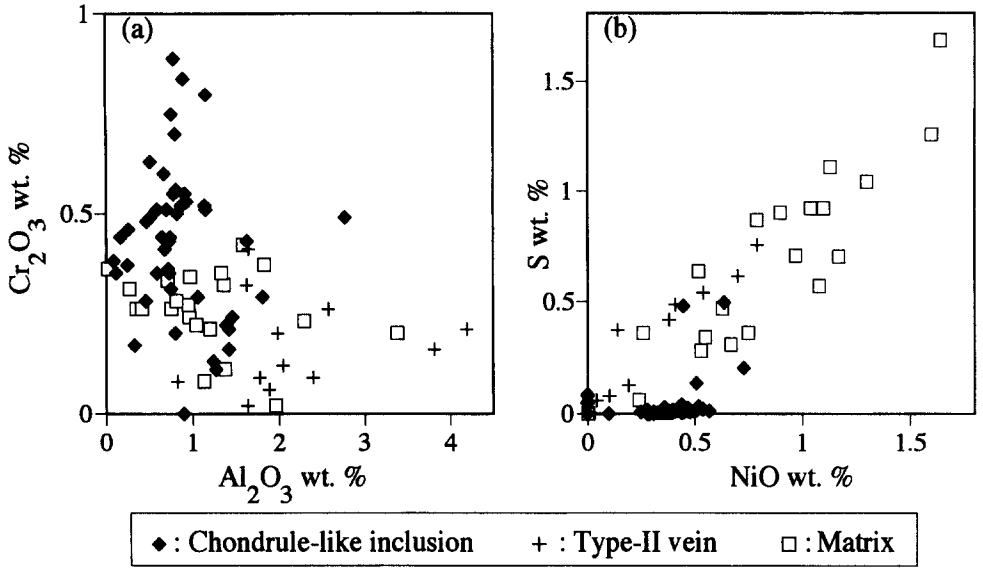

FIG. 6. Minor element contents of Fe-rich olivine in chondrule-like inclusions, matrix and veins in All-AF. Plots of wt% Cr_2O_3 vs. wt% Al_2O_3 (a), and wt% S vs. wt% NiO (b). High contents of these elements are probably due to microinclusions (see text).

is that relatively long veins (up to 4 mm) of this type penetrate several inclusions (Fig. 14a,b). Type-II veins are characterized by a layered structure (Fig. 13b); the inner layers consist of granular to anhedral grains of Fe-rich olivine (<10 μm in diameter) which resemble in morphology and composition those in the matrix of All-AF (Table 2; Fig. 6), and the outer layers consist of nepheline (<5 μm in diameter). The central portions of type-II veins are commonly hollow but are occasionally filled with salitic pyroxene (20 to 24 wt% CaO, 11 to 18 wt% FeO) (Table 3), exhibiting a pipe-like appearance on the thin sections. In rare cases, small grains of Fe sulfide occur in the central portions. The proportion of nepheline, olivine, and salitic pyroxene varies even within a vein. Generally, veins in the matrix contain a higher amount of nepheline than those in the inclusions; the latter contain more salitic pyroxene (Fig. 14b).

Table 3. Selected electron microprobe analyses of nepheline, pyroxene and andradite in Allende-AF (weight %).

	Chondrule-like inclusion		CAI-like inclusion				Matrix	Vein	
	Neph	Px	*And	Neph	Px	#Px	Neph	Neph	Px
SiO_2	43.6	53.9	36.8	42.5	53.1	48.6	43.5	41.9	49.3
Al_2O_3	34.4	3.57	1.47	33.9	1.88	2.80	34.4	35.1	0.53
TiO_2	n. d.	0.82	n. d.	0.15	n. d.	0.25	n. d.	n. d.	n. d.
FeO	1.08	0.82	25.5	1.37	7.83	9.81	1.38	0.90	17.6
MnO	n. d.	0.47	0.05	0.09	0.34	0.04	n. d.	n. d.	0.68
MgO	0.96	19.7	0.17	0.32	14.7	15.5	0.80	0.13	10.0
CaO	1.98	20.6	33.7	2.40	21.7	23.8	2.29	2.87	21.0
Na_2O	16.2	0.08	0.40	15.6	0.30	n. d.	16.1	15.8	n. d.
K_2O	1.70	n. d.	0.03	1.66	n. d.	n. d	1.70	1.91	n. d.
Cr_2O_3	0.05	0.90	n. d.	0.23	0.19	n. d	0.39	0.25	0.21
NiO	n. d.	0.22	n. d.	n. d.	n. d.	0.22	0.12	n. d.	n. d.
Total	100.0	101.1	98.1	98.2	100.0	101.0	100.7	98.9	99.3
Si	6.17	7.64	6.52	6.14	7.84	7.25	6.14	6.03	7.75
Al	5.74	0.60	0.30	5.77	0.33	2.80	5.72	5.95	0.10
Ti	n. d.	0.09	n. d.	0.02	n. d.	0.03	n. d.	n. d.	n. d.
Fe	0.13	0.10	3.78	0.17	0.97	1.22	0.16	0.11	2.31
Mn	n. d.	0.06	0.01	0.01	0.05	0.01	n. d.	n. d.	0.09
Mg	0.20	4.16	0.04	0.07	3.24	3.44	0.17	0.03	2.35
Ca	0.30	3.13	6.41	0.37	3.44	3.81	0.35	0.44	3.53
Na	4.46	0.02	0.13	4.37	0.09	n. d.	4.40	4.40	n. d.
K	0.31	n. d.	0.00	0.31	n. d.	n. d.	0.31	0.35	n. d.
Cr	0.01	0.10	n. d.	0.03	0.02	n. d	0.04	0.03	0.02
Ni	n. d.	0.03	n. d.	n. d.	n. d.	0.03	0.01	n. d.	n. d.

Neph=nepheline, Px=pyroxene, And=andradite. Atomic ratios are calculated as O=24.

* Total Fe is given as FeO.

Pyroxene in a rim of a CAI-like inclusion.

Table 4. Selected electron microprobe analyses of opaque phases in Allende-AF (weight %).

	Chondrule-like inclusion		CAI-like inclusion		
	Pent	Aw	Tro	Tro	Mag
Si	0.14	0.45	n. d.	0.16	n. d.
Fe	42.6	29.6	61.9	63.5	71.8
Co	1.19	1.98	n. d.	n. d.	n. d.
Ni	21.5	68.9	n. d.	n. d.	n. d.
P	0.47	n. d.	0.44	n. d.	n. d.
S	33.7	n. d.	37.0	37.2	n. d.
O	n. d.	n. d.	n. d.	n. d.	28.3
Total	99.6	100.9	99.3	100.9	100.1

Pent=pentlandite, Aw=awaruite, Tro=troilite, Mag=magnetite.

Within and near the thick, double-layered rim of Inclusion I-1, both type-I and type-II veins are abundant and commonly form networks (Fig. 10a,b). One of the type-II veins extends from the interior of Inclusion I-1 to the surrounding matrix, crosscutting the rim layers. The vein is nearly perpendicular to the surface of the inclusion and each of the rim layers. A type-I vein, which occurs along the boundary between the rim layers, crosscuts a type-II vein, suggesting that the type-I vein was formed after the type-II vein.

3.6. Chemical Compositions of All-AF

A major element composition of bulk All-AF obtained by EDS defocused electron beam analysis is shown in Table 1 and is also plotted in Fig. 15 with the data of All-AF reported by Palme et al. (1989). Also plotted in Fig. 15 is the bulk composition of the matrix of host Allende reported by McSween and Richardson (1977). The results of the present study are approximately consistent with the data of Palme et al. (1989), except for Ti and P (Fig. 15); Ti content is significantly higher, and P content is lower than that reported by Palme et al. (1989). Large deviations for these elements indicate that the differences in contents are probably due to heterogeneous distributions of their carrier phases (Ca-phosphate, perovskite etc.) (Table 1). Compared with bulk Allende and the matrix of host Allende, All-AF is enriched in Na and K approximately by factors of two and three, respectively. The enrichment of Na and K can be explained by the high abundance of the nepheline in All-AF. For other elements, there appear to be no significant differences between All-AF, bulk Allende, and the matrix of host Allende.

Bulk compositions of chondrule-like inclusions, CAI-like inclusions, and matrix of All-AF were also analyzed by a defocused electron beam and plotted in Fig. 16. The chondrule-like inclusions and the matrix of All-AF have closely similar compositions except that Na and P contents in the chondrule-like inclusions are much lower than in the matrix; the enrichment of Na in the matrix may be due to a higher abundance of nepheline than in the chondrule-like inclusions, and the difference in P content is probably due to heterogeneous distribution of its carrier phases. The CAI-like inclusions have very different compositions from the chondrule-like inclusions and the matrix; they are enriched in Ca, Na, S, and Ti, and depleted in Mg, Cr, and Ni. As described earlier, the differences are due to different mineral components.

FIG. 7. A chondrule-like inclusion surrounded by a thick, dark rim in plane polarized light.

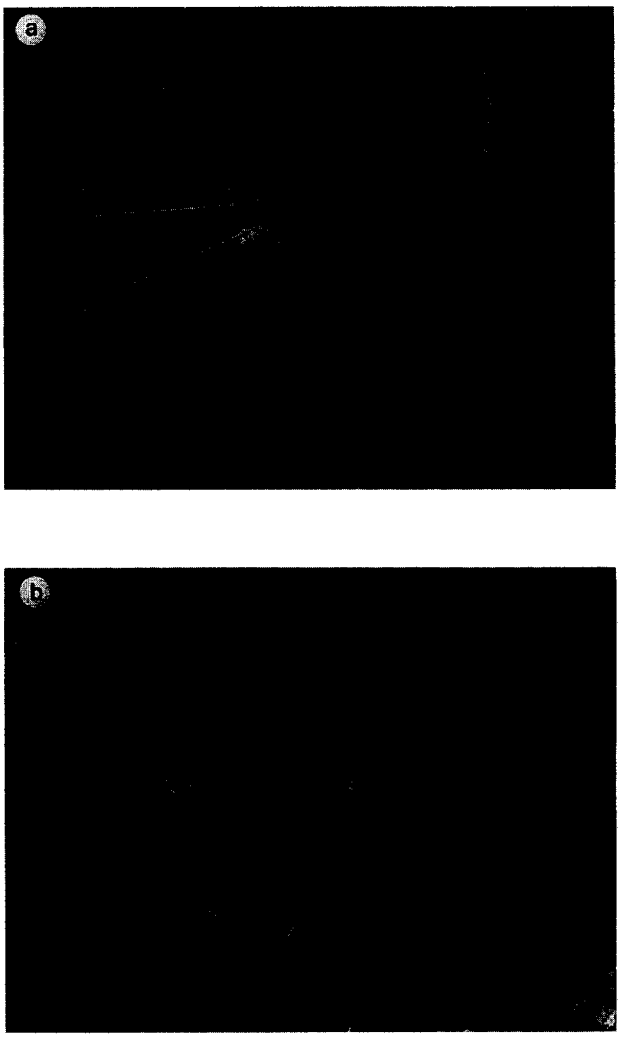

FIG. 8. (a) BSE image of a CAI-like inclusion. (b) Enlarged image of the boxed area in (a). And = andradite, Tro = troilite, Ol = Fe-rich olivine, Px = Ca-rich pyroxene, Ne = nepheline.

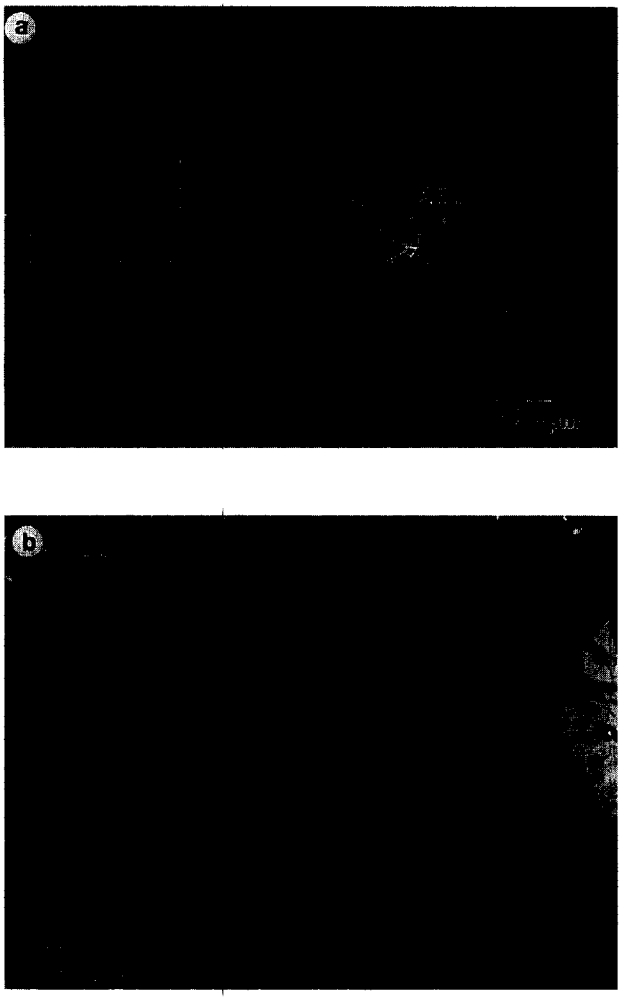

FIG. 9. (a) BSE image of a CAI-like inclusion with a halo of fibrous olivine. Abbreviations are same as Fig. 8. (b) Enlarged image of the boxed area in (a).

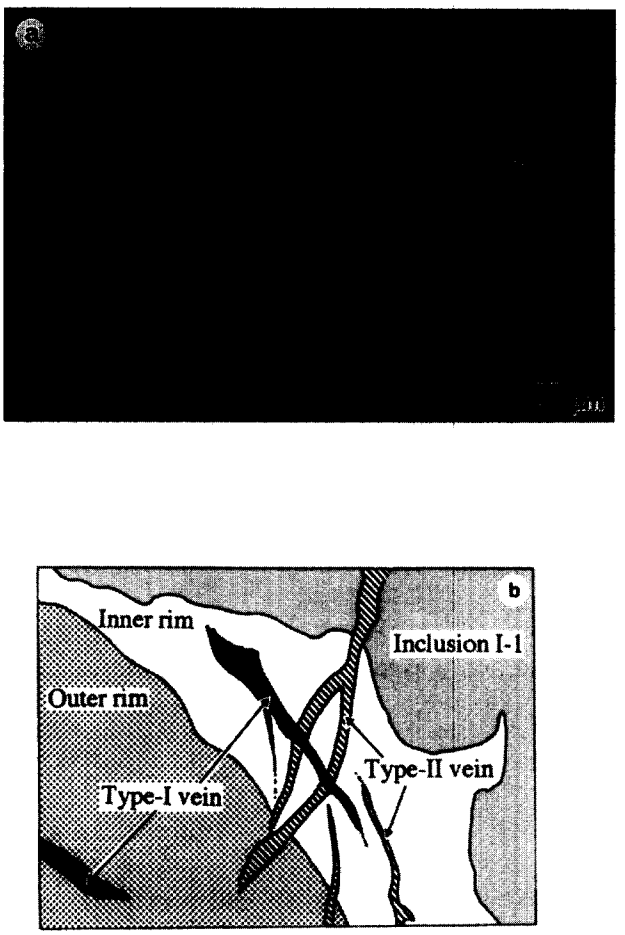

FIG. 10. (a) BSE image of a portion around Inclusion I-1. (b) Tracing of (a), showing a forked type-II vein crosscuts a double-layered rim. Also note that a type-I vein crosscuts the type-II veins.

3.7. Size Distribution of Chondrule-Like Inclusions

In order to estimate the relation between All-AF and other carbonaceous chondrite groups, we measured the sizes of chondrule-like inclusions in All-AF and compared them with those of chondrules in CM, CV, CO, and CR carbonaceous chondrites. Following the procedure of King and King (1978, 1979), apparent maximum diameter and the greatest diameter normal to the maximum diameter of each inclusion in All-AF were measured in transmitted light using a calibrated reticle.

Size frequency curves of chondrule-like inclusions in All-AF are plotted with the data of chondrules in carbonaceous chondrites obtained by King and King (1978) (Fig. 17). Maximum diameters of all the inclusions in the thin sections which have roughly rounded and oval external shapes were measured. However, some caveats should be added: (1) it was difficult to classify relatively small (<0.2 mm) inclusions in All-AF and (2) many of the inclusions of All-AF appear to have experienced deformation, thus are flattened with relatively high aspect ratios (from 1.5 to 2.0). Even if these problems are taken into consideration, we believe the comparison is valid. The results show that the size-frequency

FIG. 11. Veins (type I) filled with fine olivine grains in the periphery of Inclusion I-1 (upper right) in plane polarized light. The veins run nearly parallel to the surface of the Inclusion I-1, and some veins are connected to the inclusion. This image corresponds to the upper-left area in Fig. 2.

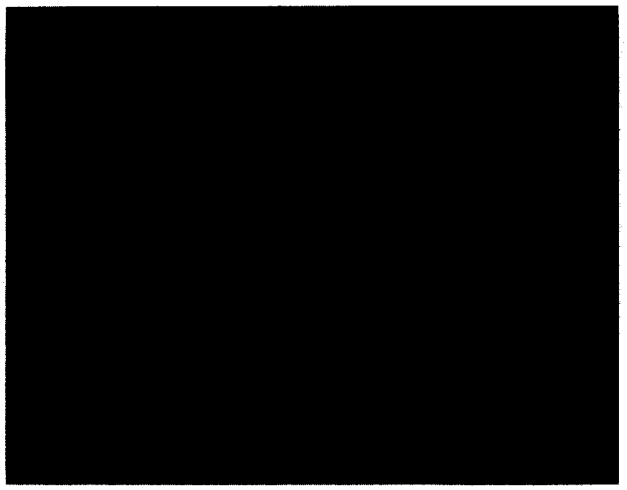

FIG. 12. High-magnification BSE image of olivine grains in the matrix of All-AF. Microinclusions of Fe-Ni sulfide (bright) are marked by arrows.

curves of chondrule-like inclusions in All-AF completely overlap with those of chondrules in CV chondrites; they are particularly similar to the curve of chondrules in Allende and are clearly distinct from those of chondrules in CM, CO, and CR (Renazzo) chondrites.

4. DISCUSSION

4.1. Formation of All-AF by Hydration and Dehydration Process

Kurat et al. (1989) interpreted that the chondrule-like inclusions, which they referred to as silicate-rich aggregates, formed by condensation from a vapor and that the textures reflect sequential aggregation of matter in the solar nebula. They further suggested that sintering, recrystallization, and partial melting could transform the inclusions into chondrules and recrystallized aggregates. However, the present study reveals abundant evidence indicating a very different origin for the inclusions. Many of the chondrule-like inclusions have peculiar textures; they are composed of assemblages of rounded to oval-shaped sections (typically 50 to 100 μm in diameter), each consisting of fine grains of Fe-rich olivine (Fig. 3a,b). Some inclusions contain bars (5 to 30 μm in width, 100 to 500 μm in length) of olivine aggregates in parallel orientation (Fig. 4a,b). Under the optical microscope, their sizes, external shapes, and internal textures are closely similar to those of chondrules, although they are different from normal chondrules in having weak birefringences and brownish translucent appearance. Most of the fine olivine grains within each rounded to oval-shaped section in the inclusions and bar have basically a common crystallographic orientation (Figs. 3b, 4a,b). It is hard to envision that small olivine particles floating in the nebula would stick to each other so that their crystallographic orientations would be so uniform. Rather, it is more likely that the rounded to oval-shaped sections and the bars had been originally large single crystals of olivine and they were transformed to aggregates of fine domains by some secondary process. In our interpretation, the rounded to oval-shaped sections and the bars of olivine aggregates in the inclusions were originally phenocrysts in porphyritic olivine chondrules and bars in barred olivine chondrules, respectively.

Similarly, the sulfide-andradite-rich inclusions were probably formed by replacement of CAIs. The presence of PGE nuggets, titanomagnetite, ilmenite, and perovskite (Kurat et al., 1989), and high contents of refractory REE (Palme et al., 1989) in the sulfide-andradite–rich inclusions in All-AF are all consistent with this interpretation. Indeed, Kurat et al. (1989) and Palme et al. (1989) suggested that the sulfide-andradite–rich inclusions represent former CAIs that experienced extensive alteration, although they proposed that the alteration reactions occurred in the solar nebula.

The presence of abundant fracture-filling veins also indicates that All-AF has been involved in secondary alteration. It is very difficult to explain the formation of the layered, pipe-like structure of type-II veins (Fig. 13b) by condensation from a nebular gas or by aggregation of dust. In particu-

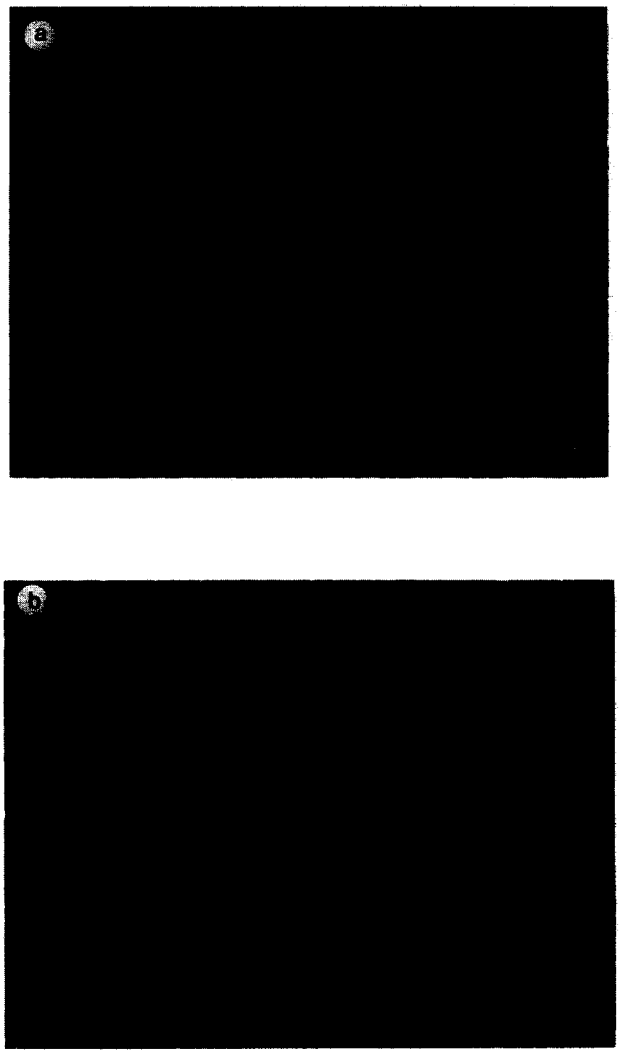

FIG. 13. (a) BSE image of a type-I vein consisting of fibrous olivine grains. (b) A type-II vein showing layered structure; inner layers composed of Fe-rich olivine (Ol), and the outer layers nepheline (Ne). Central portion is hollow and occasionally filled with salitic pyroxene (Px).

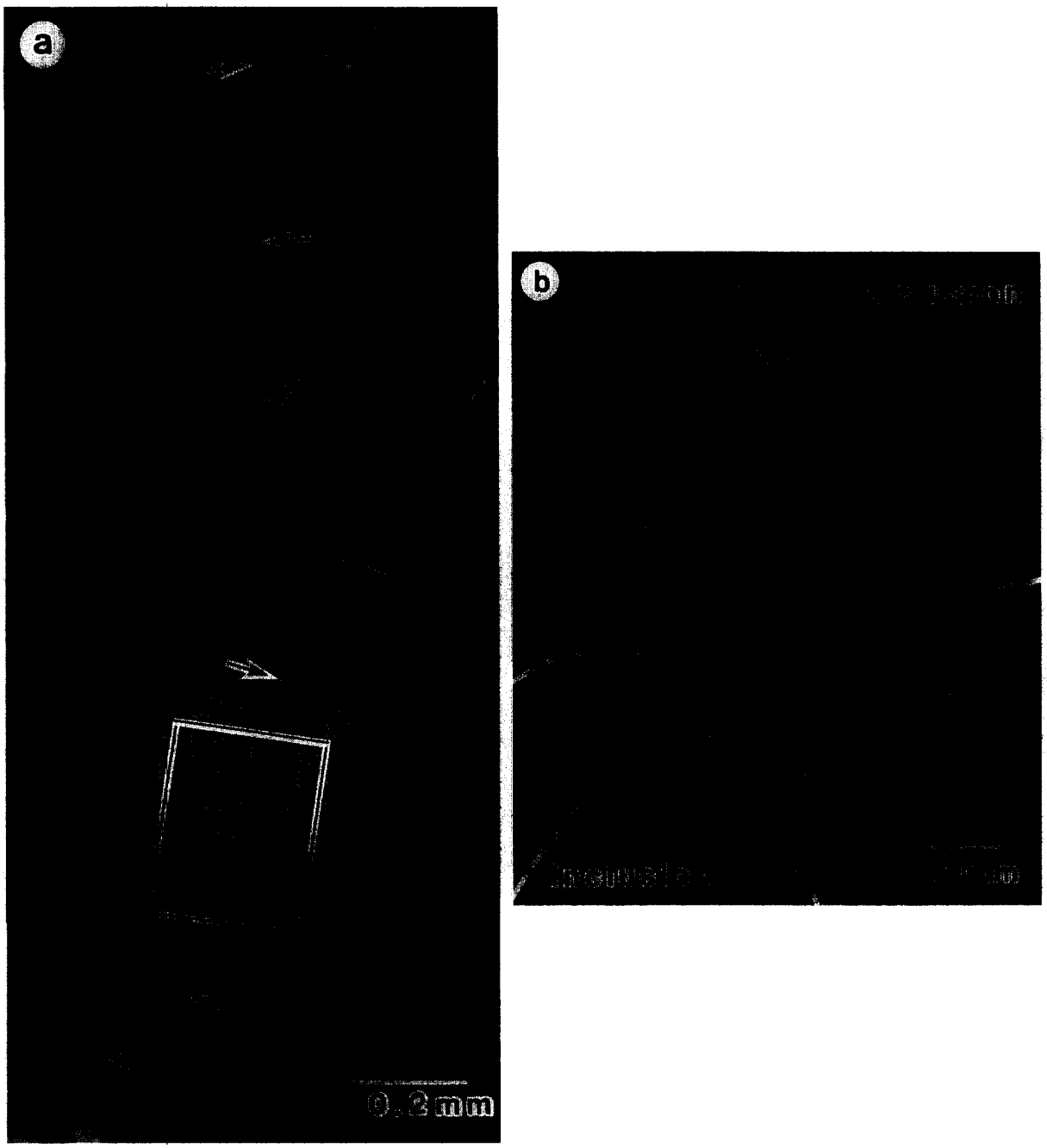

FIG. 14. (a) A photomosaic showing a long vein (type II; marked by arrows) penetrating several inclusions. (b) BSE image of the boxed area in (a). The vein (marked by small arrows), which is actually a bundle of two veins, is continuous through the boundaries between the inclusions and the matrix (broken lines). The veins are rich in salitic pyroxene (Px).

lar, we believe that the occurrence of type-II veins penetrating several inclusions (Fig. 14a,b) provides decisive evidence that secondary alteration occurred after accretion. The occurrence of type-II veins extending from the interior of Inclusion I-1 to the surrounding matrix and crosscutting the rim layers (Fig. 10a) also indicates that the veins formed after incorporation of Inclusion I-1 with the rim into the present location. The internal texture of type-I veins are very similar to the phyllosilicate veins found in the Yamato-82162 CI chondrite (Tomeoka, 1990). The veins in typical CI chondrites are regarded to have been formed by precipitation of minerals from aqueous solutions onto the walls of fractures that resulted from impacts on the meteorite parent bodies (e.g., Richardson, 1978). The type-I veins also closely resemble in texture the phyllosilicate veins produced by experimental hydrothermal alteration of Allende (Tomeoka and Kojima, 1995).

Based on these observations and evidence, we believe that All-AF has experienced secondary alteration in which aqueous solutions were involved. However, there is a serious

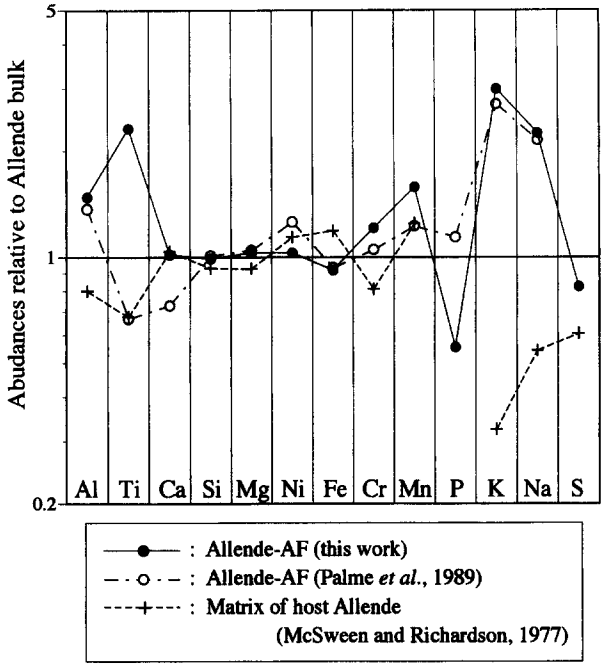

FIG. 15. Bulk chemical compositions of All-AF obtained by EDS broad beam analysis. Data are normalized to bulk Allende values referred from Jarosewich et al. (1987). Also shown are previously reported compositions of All-AF (Palme et al., 1989), and the matrix of host Allende (McSween and Richardson, 1977). The data of Palme et al. were obtained by XRF (K, Cr, Mn and Ni) and INAA (other elements).

problem that needs to be answered, i.e., why does All-AF lack minerals that are characteristic of aqueous alteration, such as phyllosilicates, sulfates, and carbonates? All-AF is entirely composed of anhydrous minerals. The same paradox

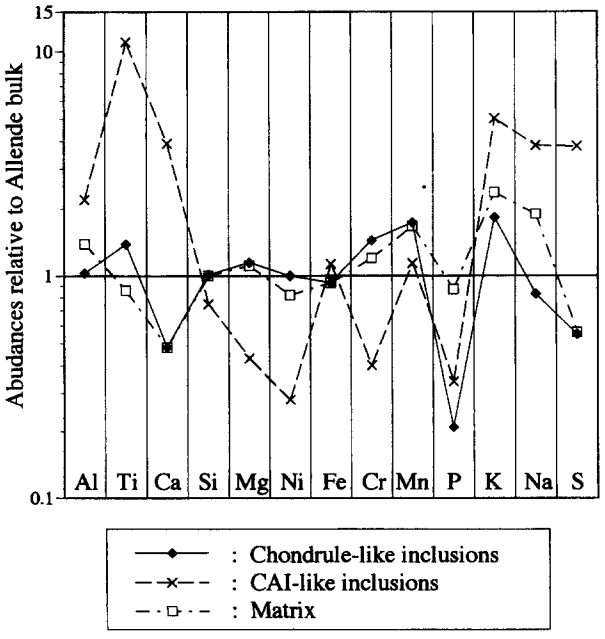

FIG. 16. Bulk compositions of chondrule-like inclusions, CAI-like inclusions and matrix of All-AF (normalized in the same way as for Fig. 15).

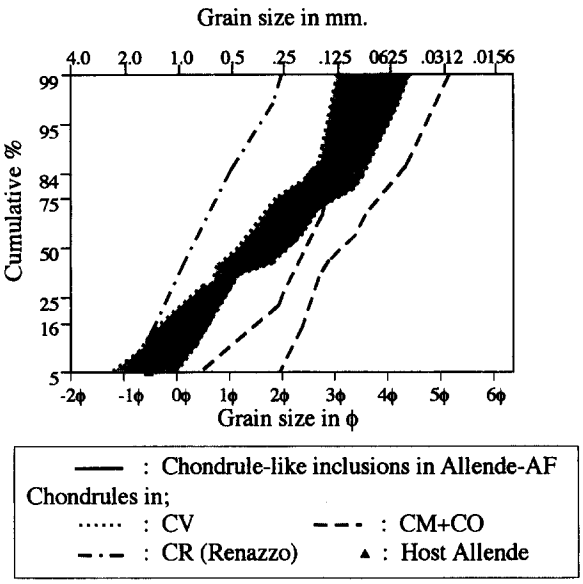

FIG. 17. Size distributions of chondrule-like inclusions in All-AF (solid line) with a cumulative probability ordinate. Also shown are data of chondrules in CM, CV, CO, CR chondrites and in Allende, referred from King and King (1978). Each pair of broken lines and dotted lines represents envelopes for CM plus CO and CV chondrites, respectively. The distribution curve of inclusions in All-AF lies in the envelope of CV chondrites (gray area).

applies to most DIs that have been reported previously, and this has been one of the major reasons why previous workers have argued against a secondary process for the origin of DIs. Regarding this problem, Kojima et al. (1993) proposed that the olivine grains constituting DIs in the Vigarano CV3 chondrite were mostly produced by dehydration and thermal transformation of phyllosilicates that had been previously formed by aqueous alteration. Based on heating experiments in vacuo, Akai (1992) reported that serpentine in the Murchison CM2 chondrite starts to transform to olivine at about 300°C and at 700°C the transformation is complete; at 750°C, olivine further transforms to enstatite. Zolensky et al. (1994) also reported that serpentine in Murchison, when heated in a H_2 atmosphere, is replaced entirely by olivine by 800°C. We believe that the interpretation of Kojima et al. (1993) can also be applied to All-AF.

Although All-AF and the matrix of host Allende consist mostly of fine grains of olivine and are similar in texture, they show several important differences in detail. Olivine grains of All-AF commonly show characteristic swirly fibrous morphologies (Figs. 9b, 13a), while such olivine grains are rare in the host Allende matrix. The fibrous olivine can be formed by thermal transformation of phyllosilicate. The experimental studies of thermal transformation of serpentine (e.g., Brindley and Zussman, 1957; Ball and Taylor, 1963; Souza Santos and Yada, 1979, 1983; Akai, 1988, 1992) showed that the transformation is basically topotactic; i.e., a pseudomorph of the fibrous serpentine is formed that contains olivine in preferred crystallographic orientations with respect to the parent serpentine crystals. TEM observations of the thermally metamorphosed CI and CM chondrites also showed that olivine transformed from phyllosilicate inherits its original fibrous morphologies (Akai, 1988, 1990;

Tomeoka et al., 1989a,b). Furthermore, All-AF contains a much higher proportion of olivine and is more homogeneous in composition than the Allende matrix, which contains, in addition to olivine, a variety of minor minerals such as low-Ca and high-Ca pyroxenes, garnets, magnetite, and Fe-Ni sulfides, etc.

Most of the olivine grains in the matrix of All-AF were found to contain numerous micro-inclusions of Fe-Ni sulfide (Fig. 12), providing additional strong evidence that the olivines in the All-AF matrix have an origin different from those in the host Allende matrix. To our knowledge, such large aggregates of olivine grains containing micro-inclusions have not been reported from any other components of carbonaceous chondrites. The micro-inclusions were probably incorporated into the olivine during thermal decomposition of a mixture of phyllosilicate, some Fe-S-Ni-rich phase such as tochilinite and sulfide, and other associated minerals. In the matrices of thermally metamorphosed CM and CI chondrites (Yamato-86720, Yamato-82162), irregularly shaped olivine grains, which were formed by transformation of phyllosilicate, intimately coexist with fine grains of Fe sulfide, Fe-Ni metal, and ferrihydrite (Tomeoka et al., 1989a,b; Akai, 1990). The general similarities between the matrices of these chondrites and the matrix olivines in All-AF containing micro-inclusions of Fe-Ni sulfide suggests that all were formed by a similar process.

The mineralogy of CAI-like inclusions is very different from those of common CAIs in CV3 and CO3 chondrites; the former are composed mainly of andradite and Fe sulfide, while the latter are composed of a variety of Ca-Al-rich phases such as melilite, spinel, anorthite, diopside, etc. During aqueous alteration of CAIs, major exchange of elements should have taken place between CAIs and surrounding matrix. In particular, Ca, Al, and Mg were presumably leached from the CAIs, while Fe and S were added. These elemental exchanges are also suggested by our recent hydrothermal experiments of Allende (Tomeoka and Kojima, 1995). The exchanges probably occurred through cracks that were produced around the boundaries between CAIs and matrix. We interpret that this is the reason why thick veins (type-I veins) are particularly abundant in the peripheries of Inclusion I-1 and other CAI-like inclusions.

Palme et al. (1989) reported that All-AF is considerably enriched in Na, K, Au, As, Sb, Br, and Hg, and slightly depleted in Ca, Ti, and Se compared with bulk Allende (also see Fig. 15). They excluded the possibility that All-AF was involved in aqueous alteration mainly because of the lack of hydrous phases. However, as mentioned above, the absence of hydrous phases can be explained by later dehydration and thermal transformation. Under hydrothermal conditions, it is known that Ca, Na, K, and Ti are particularly mobile among the major elements (McSween and Richardson, 1977), and Au and Br are also very mobile among the trace elements (Ebihara et al., 1982). Therefore, we believe it is probable that Na, K, Au, and Br were transported from elsewhere and concentrated in All-AF during aqueous alteration, while Ca and Ti were removed. We suggest the veins in All-AF served as transportation conduits, which explains why nepheline is particularly abundant in the type-II veins. Because Br is highly volatile (Fegley and Lewis, 1980), its enrichment in All-AF suggests that the subsequent thermal metamorphism occurred at relatively low temperature.

4.2. Relationship to Other Dark Inclusions

Johnson et al. (1990) reported that DIs range in texture from one endmember containing chondrules and CAIs in a matrix to the other consisting mostly of fine grains of Fe-rich olivine. Many objects so far reported as the fine-grained type of DIs in the literature appear to be similar in texture and mineralogy to All-AF (e.g., Fruland et al. 1978; Johnson et al., 1990) except for a few DIs that consist of fine-grained matrix-like material and are devoid of chondrule-like inclusions (e.g., those shown in Fig. 1e and g in Johnson et al., 1990). We think many of them could have resulted from similar alteration processes on the meteorite parent bodies. The aqueous alteration that affected All-AF should have been quite intensive and altered most of the components including chondrules, CAIs, and matrix to secondary phases, mainly phyllosilicate. However, at some stage, the aqueous alteration stopped probably because of exhaustion of water, and then, if a heat source continued to exist, thermal metamorphism occurred. Consequently, the phyllosilicate produced by aqueous alteration was dehydrated and transformed to olivine. In the case of the DIs, the thermal metamorphism probably proceeded at mild temperatures for a substantially long time, so that most of the phyllosilicate was transformed to fine grains of olivine but the coarsening and recrystallization commonly observed in metamorphosed chondrites did not occur. Assuming that the precursor phyllosilicate was serpentine, from the results of Akai (1992), we estimate that the temperature did not much exceed 300°C. Such a sequence of alteration and metamorphism might totally convert the precursor chondrite to aggregates of fine grains of nearly homogeneous olivine.

Taking such a sequence of alteration into consideration, the wide variations in texture observed in DIs can be explained by different degrees of aqueous alteration preceding thermal metamorphism. Kojima and Tomeoka (1995) recently studied two other DIs in Allende, which are distinct in mineralogy and texture from each other. One of the DIs is composed mostly of fine grains of olivine, petrographically similar to All-AF, whereas the other DI contains chondrules composed of coarse grains of Mg-rich olivine and pyroxene embedded in a fine-grained matrix. The former DI was probably involved in intense aqueous alteration like All-AF. In contrast, the latter DI may have experienced only a minor degree of aqueous alteration; thus, only chondrule mesostases and some portions of matrix were affected, but phenocrysts in chondrules largely survived the aqueous alteration.

It is interesting to note that the oxygen isotopic compositions of DIs correlate with petrographic variations (Johnson et al., 1990). DIs form linear arrays on the three oxygen isotope diagram with slopes slightly shallower than the slope of the refractory inclusion mixing line. The chondrule-bearing varieties of DIs plot on the lower end of the DI array nearest the bulk CV3 values, while the fine-grained varieties have more ^{16}O-depleted compositions with some plotting near the matrix of the Murchison CM chondrite. All-AF is among the most ^{16}O-depleted DIs from Allende (Palme et al., 1989). Murchison and other CM chondrites are believed

to have become depleted in ^{16}O by reaction with aqueous solutions (Clayton and Mayeda, 1984). We are currently uncertain why DIs plot on a steeper slope than that of CM and CI chondrites, but the fact that fine-grained DIs are more ^{16}O-depleted than chondrule-bearing ones would suggest that the former experienced more intensive aqueous alteration than the latter.

It is also probable that there was a range in the degree of subsequent thermal metamorphism of DIs. Ivanov et al. (1994) reported that a clast in the Kaidun meteorite contains rounded objects very similar to the chondrule-like inclusions in All-AF. The rounded objects consist of fine grains of olivine, clinopyroxene, and phyllosilicate, and a phyllosilicate-sulfide vein was also found in the same clast. Kracher et al. (1985) reported "ghosts" of chondrules and CAIs in a DI in the Leoville CV3 chondrite. The "ghosts" contain phyllosilicate-like, but apparently dehydrated, materials with an olivine-like composition. These clasts in Kaidun and Leoville appear to be a kind of DIs that experienced intense aqueous alteration like All-AF, followed by less intense thermal metamorphism.

4.3. CV Parent Body Implied by Allende-AF and Other DIs

It has been commonly accepted that the CV and CO chondrites have escaped major degrees of aqueous alteration and thermal metamorphism. From the size distribution of the chondrule-like inclusions (Fig. 17) and the abundance of CAI-like inclusions, the precursor of All-AF is likely to have been a CV type material, probably Allende itself. Oxygen isotopic and chemical compositions, including trace elements (Palme et al., 1989), are consistent with this interpretation. If this is true, All-AF provides evidence that aqueous alteration and thermal metamorphism have occurred on the CV parent body. The aqueous alteration that affected All-AF should have been sufficiently intensive to completely transform coarse-grained olivine and pyroxene in chondrules to phyllosilicates. Therefore, it is plausible that the CV parent body was not a homogeneous, dry, and quiet body as has been implicitly imagined, but rather was a heterogeneous dynamic body in which aqueous alteration and thermal metamorphism occurred actively. However, the aqueous alteration and thermal metamorphism must not have extended throughout the CV parent body, but occurred locally in the body where water and heat were available. Thus, CV materials located where water could not have penetrated remained unaltered, and most of CV chondrites that we have came from such a relatively dry, unmetamorphosed place.

If All-AF was really derived from the Allende parent body, host Allende itself also may not have escaped such secondary process. Several previous workers have reported that some chondrules and CAIs in Allende contain minor amounts of phyllosilicates (Tomeoka and Buseck, 1982a,b; Hashimoto and Grossman, 1987), and there is indeed evidence that a phyllosilicate was formed by alteration of olivine (Fig. 3 in Tomeoka and Buseck, 1982b). A thermoluminescence sensitivity measurement indicated that Allende is classified to petrographic subtype 3.2 (Guimon et al., 1995). Matrix olivine in Allende is very homogeneous compared to those in other CV chondrites (Peck, 1983), and in places shows fine fibrous morphology similar to the olivine in All-AF. In many Allende chondrules, mesostasis glass is altered to nepheline (e.g., Kimura and Ikeda, 1995), and Mg-rich olivine has fayalite-rich rims (e.g., Peck and Wood, 1987; Hua et al., 1988). Tomeoka and Kojima (1995) recently showed that olivines in chondrules in hydrothermally treated Allende are enriched in Fe at their edges, suggesting that the fayalite-rich rims of chondrule olivines could have formed during aqueous alteration.

In this regard, we also point out that a part of the rim surrounding All-AF is distinctly enriched in Fe-Ni sulfide particles; the part of the rim is right next to the large Inclusion I-1 which contains particularly abundant Fe-Ni sulfides (See section 3.3). The enrichment of Fe-Ni sulfide particles can be ascribed to diffusion of Fe, S, and Ni from Inclusion I-1. This suggests that thermal metamorphism occurred to some extent after incorporation of All-AF with the rim to the present location. All of these observations and evidence suggest that host Allende may have been locally affected by minor aqueous alteration and subsequent thermal dehydration. If so, it would be necessary to substantially re-evaluate a number of previous interpretations developed for the origin of Allende components such as CAIs and matrix.

While we believe our data and observations support the Allende parent body as the source of All-AF, we cannot exclude the possibility that it came from generally similar, but perhaps more aqueously altered, parent body. Recent transmission electron microscope studies (e.g., Keller and Buseck, 1990; Tomeoka and Buseck, 1990; Keller and McKay, 1993; Zolensky et al., 1993; Keller et al., 1994) indicate that some other CV3 chondrites (Kaba, Mokoia, Grosnaja, Vigarano, and Bali) were more or less affected by aqueous alteration. Keller et al. (1994) reported that the Bali CV3 chondrite has undergone deformation and aqueous alteration, and that it consists of two different regions, i.e., least-altered and heavily altered regions. In heavily altered regions, the majority of chondrules and inclusions are largely replaced by phyllosilicates, appearing pale tan in transmitted light. The appearance in transmitted light and the ^{16}O-depleted isotopic composition of the heavily altered regions of Bali suggest that they are related to All-AF and other fine-grained DIs.

Besides DIs in CV chondrites, many carbonaceous chondrite-like xenoliths have been reported in both primitive and differentiated meteorites, and most of them resemble CM chondrites (Table 2 in Wasson and Wetherill, 1979). Dehydration of phyllosilicates is also observed in such carbonaceous chondrite xenoliths (e.g., Fodor and Keil, 1976; Barber and Hutchison, 1991; Zolensky et al., 1992; Buchanan et al., 1993). As the DIs and xenoliths were incorporated as clasts, they probably resided near the surfaces of the meteorite parent bodies where brecciation actively occurred. This is consistent with the model by Grimm and McSween (1989) that aqueous alteration occurred in a regolith. It would be significant to note that the surfaces of most of C, G, B, and F asteroids show reflectance spectra very similar to thermally metamorphosed CI-CM-like materials (Hiroi et al., 1993, 1995). Therefore, it is plausible that the sequence of secondary process, i.e., aqueous alteration and subsequent thermal metamorphism, is a common event that occurred on primitive asteroids. We believe that All-AF and other DIs preserve

records of secondary processes on their meteorite parent bodies, and that further systematic studies of DIs would provide more information regarding the evolution of carbonaceous chondrite parent bodies.

5. CONCLUSIONS

1) All-AF is composed essentially of fine grains of Fe-rich olivine and appears to be closely related to the fine-grained variety of DIs. All-AF was previously interpreted to be a primary aggregate of direct condensates in the solar nebula (Kurat et al., 1989; Palme et al., 1989). However, our re-examination strongly suggests that it has resulted from intense aqueous alteration and subsequent thermal metamorphism on the meteorite parent body. The rounded to oval-shaped inclusions in All-AF show internal textures suggesting that they are pseudomorphs after porphyritic or barred olivine chondrules. Some inclusions appear to be highly altered CAIs. All-AF contains abundant veins that are filled with fine grains of olivine. Some of the veins penetrate several chondrule-like inclusions, providing decisive evidence that the veins were formed after accretion.
2) Although both All-AF and matrix of host Allende consist largely of Fe-rich olivine, olivines in the former commonly exhibit characteristic fibrous morphologies distinct from those in the latter. Olivine grains in the matrix of All-AF contain numerous micro-inclusions of Fe-Ni sulfide. Most of the olivines in All-AF were probably formed by dehydration and thermal transformation of phyllosilicate. The fibrous morphologies of olivines in veins and inclusions suggest that they are pseudomorphs after phyllosilicate. The micro-inclusions of Fe-Ni sulfide may have been incorporated into the olivine during thermal decomposition of a mixture of phyllosilicate and Fe-S-Ni-rich phases such as tochilinite and sulfide.
3) The size distribution of chondrule pseudomorphs and the abundance of CAI pseudomorphs suggest that the precursor of All-AF is a CV chondrite, probably Allende itself. Oxygen isotopic and chemical compositions support this view. Therefore, the present study suggests that extensive aqueous alteration and thermal metamorphism occurred locally on the CV parent body, probably near the surface. Most of CV chondrites that we have probably came from a relatively dry, unmetamorphosed part of the parent body. If our view is correct, it may be necessary to reevaluate much of the previous interpretations of the origin and the formation process of CV chondrites which have overwhelmingly emphasized primary nebular processes.
4) Many other previously studied DIs are similar in texture and mineralogy to All-AF and appear to have experienced similar secondary process on the meteorite parent bodies. The wide variations in texture of DIs can be explained by different degrees of aqueous alteration that preceded thermal metamorphism. The sequence of secondary process, i.e., aqueous alteration and subsequent thermal metamorphism, may not have been restricted to CV parent bodies but may have been a common event that occurred on parent bodies of other carbonaceous-chondrite types. We believe that further systematic studies of DIs will provide a more precise picture of the evolution of primitive parent bodies.

Acknowledgments—We greatly thank Dr. G. Kurat, Naturhistorisches Museum, for his generosity to provide us with the samples of All-AF and thus to give us the opportunity of studying this fascinating sample. We also thank Drs. H. Palme and H. Takeda for useful discussions. Thoughtful and constructive reviews by Drs. L. P. Keller, D. W. Mittlefehldt, M. K. Weisberg, and M. E. Zolensky are gratefully acknowledged. Scanning electron microscopy was performed at the Mineralogical Institute and Geological Institute, University of Tokyo, and at the Department of Earth and Planetary Sciences, Kobe University. This study was supported by the Grant-in-Aid of the Japan Ministry of Education, Science and Culture (No. 06403001), and by Research Fellowship of the Japan Society for the Promotion of Science for Young Scientists.

Editorial handling: D. W. Mittlefehldt

REFERENCES

Akai J. (1988) Incompletely transformed serpentine-type phyllosilicates in the matrix of Antarctic CM chondrites. *Geochim. Cosmochim. Acta* **52,** 1593–1599.

Akai J. (1990) Mineralogical evidence of heating events in Antarctic carbonaceous chondrites, Y-86720 and Y-82162. *Proc. NIPR Symp. Antarct. Meteorites* **3,** 55–68.

Akai J. (1992) T-T-T diagram of serpentine and saponite, and estimation of metamorphic heating degree of Antarctic carbonaceous chondrites. *Proc. NIPR Symp. Antarct. Meteorites* **5,** 120–135.

Ball M. C. and Taylor H. F. (1963) The dehydration of chrysotile in air and under hydrothermal conditions. *Mineral. Mag.* **33,** 467–482.

Barber D. J. and Hutchison R. (1991) The Bencubbin stony-iron meteorite breccia: Electron petrography, shock history and affinities of a "carbonaceous chondrite" clast. *Meteoritics* **26,** 83–95.

Bischoff A., Palme H., Spettel B., Clayton R. N., and Mayeda T. K. (1988) The chemical composition of dark inclusions from the Allende meteorite. *Lunar Planet. Sci. XIX,* 88–89 (abstr.).

Brindley G. W. and Zussman J. (1957) A structural study of the thermal transformation of serpentine minerals to forsterite. *Amer. Mineral.* **42,** 461–474.

Buchanan P. C., Zolensky M. E., and Reid A. M. (1993) Carbonaceous chondrite clasts in the howardites Bholghati and EET87513. *Meteoritics* **28,** 659–682.

Bunch T. E. and Chang S. (1979) Thermal metamorphism (shock?) and hydrothermal alteration in CV3 meteorites. *Lunar Planet. Sci. X,* 164–166 (abstr.).

Bunch T. E. and Chang S. (1983) Allende dark inclusions: Samples of primitive regoliths. *Lunar Planet. Sci. XIV,* 75–76 (abstr.).

Clayton R. N. and Mayeda T. K. (1984) The oxygen isotope record in Murchison and other carbonaceous chondrite. *Earth Planet. Sci. Lett.* **67,** 151–161.

Ebihara M., Wolf R., and Anders E. (1982) Are CI chondrites chemically fractionated? A trace element study. *Geochim. Cosmochim. Acta* **46,** 1849–1861.

Fegley B., Jr. and Lewis J. S. (1980) Volatile element chemistry in the solar nebula: Na, K, F, Cl, Br, and P. *Icarus* **41,** 439–455.

Fodor R. V. and Keil K. (1976) Carbonaceous and non-carbonaceous lithic fragments in the Plainview, Texas, chondrite: Origin and history. *Geochim. Cosmochim. Acta* **40,** 177–189.

Fruland R. M., King E. A., and McKay D. S. (1978) Allende dark inclusions. *Proc. 9th Lunar Planet. Sci. Conf.,* 1305–1329.

Grimm R. E. and McSween H. Y., Jr. (1989) Water and the thermal evolution of carbonaceous chondrite parent bodies. *Icarus* **82,** 244–280.

Guimon R. K., Symes S. J. K., Sears D. W. G., and Benoit P. H. (1995) Chemical and physical studies of type 3 chondrites. XII: The metamorphic history of CV chondrites and their components. *Meteoritics* **30,** 704–714.

Hashimoto A. and Grossman L. (1987) Alteration of Al-rich inclusions inside amoeboid olivine aggregates in the Allende meteorite. *Geochim. Cosmochim. Acta* **51,** 1685–1704.

Hiroi T., Pieters C. M., Zolensky M. E., and Lipschutz M. E. (1993) Evidence of thermal metamorphism on the C, G, B, and F asteroids. *Science* **261,** 1016–1018.

Hiroi T., Pieters C. M., Zolensky M. E., and Lipschutz M. E. (1995) Thermal metamorphism of the C, G, B, and F asteroids seen from the 3-μm absorption band in comparison with carbonaceous chondrites. *Papers presented to the twentieth Symp. Antarct. Meteorites,* 72–75 (abstr.).

Hua X., Adam J., Palme H., and El Goresy A. (1988) Fayalite-rich rims, veins, and halos around and in forsteritic olivines in CAIs and chondrules in carbonaceous chondrites: Types, compositional profiles and constraints of their formation. *Geochim. Cosmochim. Acta* **52,** 1389–1408.

Ivanov A. V., Zolensky M. E., Brandstätter F., Kurat G., and Kononkova N. N. (1994) A phyllosilicate-sulfide vein in Kaidun. *Meteoritics* **29,** 477 (abstr.).

Jarosewich E., Clark R. S., Jr., and Barrows J. N. (1987) The Allende Meteorite Reference Sample. *Smithson. Contrib. Earth Sci.* **27,** 1–49.

Johnson C. A., Prinz M., Weisberg M. K., Clayton R. N., and Mayeda T. K. (1990) Dark inclusions in Allende, Leoville, and Vigarano: Evidence for nebular oxidation of CV3 constituents. *Geochim. Cosmochim. Acta* **54,** 819–830.

Keller L. P. and Buseck P. R. (1990) Aqueous alteration in the Kaba CV3 carbonaceous chondrite. *Geochim. Cosmochim. Acta* **54,** 2113–2120.

Keller L. P. and McKay D. S. (1993) Aqueous alteration of the Grosnaja CV3 carbonaceous chondrite. *Meteoritics* **28,** 378 (abstr.).

Keller L. P., Thomas K. L., Clayton R. N., Mayeda T. K., DeHart J. M., and McKay D. S. (1994) Aqueous alteration of the Bali CV3 chondrite: Evidence from mineralogy, mineral chemistry, and Oxygen isotopic compositions. *Geochim. Cosmochim. Acta* **58,** 5589–5598.

Kimura M. and Ikeda Y. (1995) Anhydrous alteration of Allende chondrules in the solar nebula II: Alkali-Ca exchange reactions and formation of nepheline, sodalite and Ca-rich phases in chondrules. *Proc. NIPR Symp. Antarct. Meteorites* **8,** 123–138.

King T. V. V. and King E. A. (1978) Grain size and petrography of C2 and C3 carbonaceous chondrites. *Meteoritics* **13,** 47–72.

King T. V. V. and King E. A. (1979) Size frequency distributions of fluid drop chondrules in ordinary chondrites. *Meteoritics* **14,** 91–96.

Kojima T. and Tomeoka K. (1993) An unusual dark clast in Allende: Possible product of parent body process. *Papers presented to the eighteenth Symp. Antarct. Meteorites,* 12–14 (abstr.).

Kojima T. and Tomeoka K. (1994) Evidence for aqueous alteration and thermal metamorphism in a dark clast found in Allende. *Meteoritics* **29,** 484 (abstr.).

Kojima T. and Tomeoka K. (1995) Textural variations of dark inclusions in Allende CV3 chondrite. *Papers presented to the twentieth Symp. Antarct. Meteorites,* 115–117 (abstr.).

Kojima T., Tomeoka K., and Takeda H. (1993) Unusual dark clasts in the Vigarano CV3 carbonaceous chondrite: Record of parent body process. *Meteoritics* **28,** 649–658.

Kracher A., Keil K., Kallemeyn G. W., Wasson J. T., Clayton R. N., and Huss G. I. (1985) The Leoville (CV3) accretionary breccia. *Proc. 16th Lunar Planet. Sci. Conf.,* D123–D135.

Kurat G., Palme H., Brandstätter F., and Huth J. (1989) Allende xenolith AF: Undisturbed record of condensation and aggregation of matter in the Solar Nebula. *Z. Naturforsch.* **44a,** 988–1004.

McSween H. Y., Jr., and Richardson S. M. (1977) The composition of carbonaceous chondrite matrix. *Geochim. Cosmochim. Acta* **41,** 1145–1161.

Metzler K., Bischoff A., and Stöffler D. (1992) Accretionary dust mantles in CM chondrites: Evidence for solar nebula process. *Geochim. Cosmochim. Acta* **56,** 2873–2897.

Palme H., Kurat G., Spettel B., and Burghele A. (1989) Chemical composition of an unusual xenolith of the Allende meteorite. *Z. Naturforsch.* **44a,** 1005–1014.

Peck J. A. (1983) Chemistry of CV3 matrix minerals and Allende chondrule olivine. *Meteoritics* **18,** 373–374 (abstr.).

Peck J. A. and Wood J. A. (1987) The origin of ferrous zoning in Allende chondrule olivine. *Geochim. Cosmochim. Acta* **51,** 1503–1510.

Richardson S. M. (1978) Vein formation in the CI carbonaceous chondrites. *Meteoritics* **13,** 141–159.

Souza Santos H. and Yada K. (1979) Thermal transformation of chrysotile studies by high resolution electron microscopy. *Clays Clay Mineral.* **27,** 161–174.

Souza Santos H. and Yada K. (1983) Thermal transformation of antigorite as studied by electron optical method. *Clays Clay Mineral.* **31,** 241–250.

Tomeoka K. (1990) Phyllosilicate veins in a CI meteorite: Evidence for aqueous alteration on the parent body. *Nature* **345,** 138–140.

Tomeoka K. and Buseck P. R. (1982a) Intergrown mica and montmorillonite in the Allende carbonaceous chondrite. *Nature* **299,** 326–327.

Tomeoka K. and Buseck P. R. (1982b) An unusual layered mineral in chondrules and aggregates of the Allende carbonaceous chondrite. *Nature* **299,** 327–329.

Tomeoka K. and Buseck P. R. (1990) Phyllosilicates in the Mokoia CV carbonaceous chondrite: Evidence for aqueous alteration in an oxidizing environment. *Geochim. Cosmochim. Acta* **54,** 1745–1754.

Tomeoka K. and Kojima T. (1995) Aqueous alteration of the Allende CV3 chondrite: A hydrothermal experiment. *Papers presented to the twentieth Symp. Antarct. Meteorites,* 251–253 (abstr.).

Tomeoka K., Kojima H., and Yanai K. (1989a) Yamato-82162: A new kind of CI carbonaceous chondrite found in Antarctica. *Proc. NIPR Symp. Antarct. Meteorites* **2,** 36–54.

Tomeoka K., Kojima H., and Yanai K. (1989b) Yamato-86720: A CM carbonaceous chondrite having experienced extensive aqueous alteration and thermal metamorphism. *Proc. NIPR Symp. Antarct. Meteorites* **2,** 55–74.

Wasson J. T. and Wetherill G. W. (1979) Dynamical, chemical and isotopic evidence regarding the formation locations of asteroids and meteorites. In *Asteroids* (ed. T. Gehrels), pp. 926–974. Univ. Arizona Press.

Zolensky M. E., Weisberg M. K., Buchanan P. C., Prinz M., Reid A., and Barrett R. A. (1992) Mineralogy of dark clasts in CR chondrites, eucrites, and howardites. *Lunar Planet. Sci. XXIII,* 1587–1588 (abstr.).

Zolensky M. E., Barret R., and Browning L. (1993) Mineralogy and compositions of matrix and chondrule rims in carbonaceous chondrites. *Geochim. Cosmochim. Acta* **57,** 3123–3148.

Zolensky M. E., Lipschutz M. E., and Hiroi T. (1994) Mineralogy of artificially heated carbonaceous chondrites. *Lunar Planet. Sci. XXV,* 1567–1568 (abstr.).